

See discussions, stats, and author profiles for this publication at: <https://www.researchgate.net/publication/235326012>

Ultrafast Photoinduced Energy and Electron Transfer in Multi-Modular Donor-Acceptor Conjugates

DATASET *in* CHEMISTRY · FEBRUARY 2013

Impact Factor: 5.73

CITATIONS

2

READS

31

6 AUTHORS, INCLUDING:



Mohamed E El-Khouly

Kafrelsheikh University

129 PUBLICATIONS 3,161 CITATIONS

SEE PROFILE



Volodymyr V Nesterov

New Mexico Highlands University

318 PUBLICATIONS 1,383 CITATIONS

SEE PROFILE



Melvin E Zandler

Wichita State University

107 PUBLICATIONS 3,339 CITATIONS

SEE PROFILE

Ultrafast Photoinduced Energy and Electron Transfer in Multi-Modular Donor–Acceptor Conjugates

Mohamed E. El-Khouly,^[a, e] Channa A. Wijesinghe,^[b] Vladimir N. Nesterov,^[c]
Melvin E. Zandler,^[b] Shunichi Fukuzumi,^{*, [a, d]} and Francis D'Souza^{*, [c]}

Abstract: New multi-modular donor–acceptor conjugates featuring zinc porphyrin (ZnP), catechol-chelated boron dipyrin (BDP), triphenylamine (TPA) and fullerene (C₆₀), or naphthalenediimide (NDI) have been newly designed and synthesized as photosynthetic antenna and reaction-center mimics. The X-ray structure of triphenylamine-BDP is also reported. The wide-band capturing polyad revealed ultrafast energy-transfer ($k_{\text{ENT}} = 1.0 \times 10^{12} \text{ s}^{-1}$) from the singlet excited BDP to the covalently linked ZnP owing to close proximity

and favorable orientation of the entities. Introducing either fullerene or naphthalenediimide electron acceptors to the TPA-BDP-ZnP triad through metal–ligand axial coordination resulted in electron donor–acceptor polyads whose structures were revealed by spectroscopic, electrochemical and

computational studies. Excitation of the electron donor, zinc porphyrin resulted in rapid electron-transfer to coordinated fullerene or naphthalenediimide yielding charge separated ion-pair species. The measured electron transfer rate constants from femtosecond transient spectral technique in non-polar toluene were in the range of 5.0×10^9 – $3.5 \times 10^{10} \text{ s}^{-1}$. Stabilization of the charge-separated state in these multi-modular donor–acceptor polyads is also observed to certain level.

Keywords: donor–acceptor systems • electron transfer • energy transfer • fullerene • artificial photosynthesis

Introduction

The capability of photosynthetic reaction center to harvest sunlight and convert that into chemical energy using basic chemical ingredients^[1] has inspired research on artificial photosynthesis^[2–8] that has led to the developments of pho-

tovoltaics, optoelectronics and photocatalysis.^[9–14] The complex events of photosynthesis include wide-band light capture and funneling by the antenna entities, and charge separation and migration resulting into long-lived charge separated states at the reaction center.^[1] A variety of donor and acceptor molecules, covering different portions of the electromagnetic spectrum and having different redox states are being utilized in an effort to capture most of the useful sunlight from the visible-near IR portion, ultimately resulting into long-lived charge separated states.^[2–8] The delocalization of charges within the spherical carbon structure of the rigid aromatic π -sphere of fullerenes^[15] has captured special attention.^[4,5,7] The small reorganization energies of fullerenes in electron-transfer reactions resulted in fast charge separation and relatively slow charge recombination yielding long-lived charge separated states.^[16–19] When simple donor–acceptor dyads were appended with additional photo- or redox active molecules resulted in polyads (triads, tetrads, etc.) capable of undergoing sequential energy or electron or combination of these photochemical events. The polyads have also been utilized to build photovoltaic devices and successful conversion of light into electricity has been demonstrated,^[4,5,7] revealing the importance of building polyads of different donor and acceptor entities for solar energy-harvesting applications.^[8,20] The use of non-covalent interactions, such as metal–ligand coordination, electrostatic effects and hydrogen bonds, has provided a much easier means of constructing electron donor–acceptor supramolecular ensembles that could mimic the function of the photosynthetic reaction center.^[6–8,19,20] However, construction of polyads by


[a] Dr. M. E. El-Khouly, Prof. S. Fukuzumi
Department of Material and Life Science
Graduate School of Engineering
Osaka University, Suita, Osaka 565-0871 (Japan)
Fax: (+81) 6-6879-7370
E-mail: fukuzumi@chem.eng.osaka-u.ac.jp

[b] Dr. C. A. Wijesinghe, Prof. M. E. Zandler
Department of Chemistry, Wichita State University
Wichita, KS 67260-0051 (USA)

[c] Dr. V. N. Nesterov, Prof. F. D'Souza
Department of Chemistry, University of North Texas
1155 Union Circle, 305070, Denton, TX 76203-5017 (USA)
Fax: (+1) 940-565-4318
E-mail: Francis.DSouza@unt.edu

[d] Prof. S. Fukuzumi
Department of Bioinspired Science
Ewha Womans University, Seoul 120-750 (Korea)

[e] Dr. M. E. El-Khouly
Current address: Department of Chemistry
Faculty of Science, Kafr el-Sheikh University (Egypt)

 Supporting information for this article (including X-ray structural data and crystal packing diagram of the triphenylamine-boron dipyrin dyad, cyclic voltammograms of the studied compounds, optical titration curves for donor–acceptor formation, MALDI-MS, and nano-second transient data of control compounds) is available on the WWW under <http://dx.doi.org/10.1002/chem.201202265>.

combination of covalent and non-covalent bonding has still remained a challenge.

In the present study, we have assembled new molecular polyads using molecular entities combined by covalent and non-covalent bonding revealing absorption of light at different parts of the spectrum, and at the same time, funneling the absorbed energy to the primary electron donor center. Such excitation transfer, as a result of matching of energy levels of different entities, is of paramount importance to exploit energy from a wide spectral region. The structures of the investigated triads are shown in Figure 1 a and b, where-

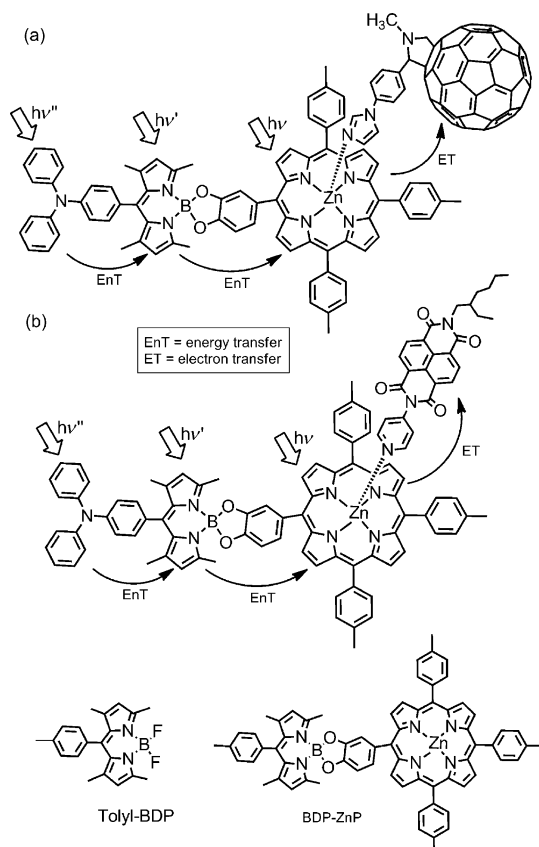


Figure 1. Structures of the multi-modular donor-acceptor polyads featuring (a) triphenylamine, BDP, ZnP and imidazole functionalized fullerene ($C_{60}Im$), and (b) triphenylamine, BDP, ZnP and pyridine appended naphthalenediimide (NDIpy) to probe photoinduced sequential energy- and electron-transfer events.

as compounds labeled as Tolyl-BDP and BDP-ZnP are control compounds. The covalently linked triad features TPA, BDP, and ZnP entities are positioned in such a fashion that excitation of either TPA or BDP results in ultrafast transfer of energy to the terminal energy acceptor and electron donor, ZnP. In the presence of either one of the electron acceptor (fullerene or naphthalenediimide), which is combined with ZnP by the coordination bond, results in photoinduced electron-transfer generating charge-separated states. The photochemical events in these new polyads have been investigated using the femtosecond transient absorption technique in nonpolar toluene, keeping in consideration that the

protein environment surrounding the photosynthetic reaction center is nonpolar with a low dielectric constant.

Results and Discussion

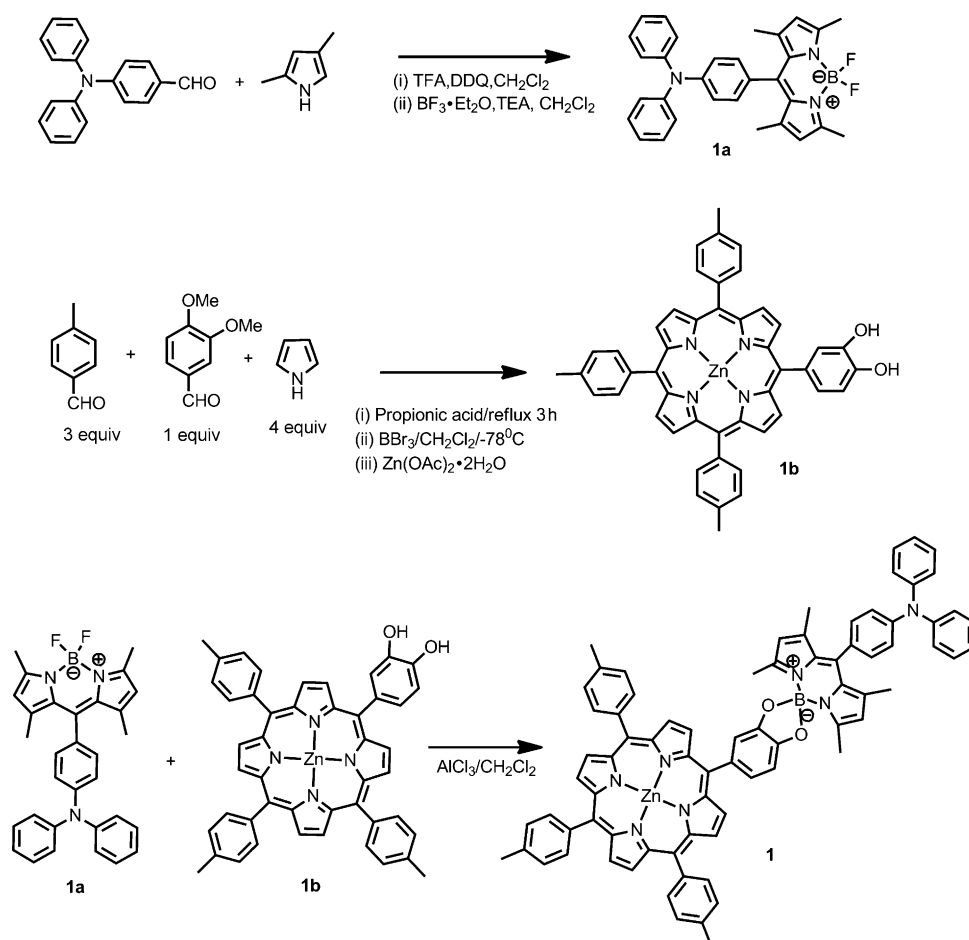
Synthesis of TPA-BDP-ZnP triad, 1: The synthesis of TPA-BDP-ZnP triad (**1**) was accomplished by using a multi-step procedure as shown in Scheme 1. For this, first, 4-(diphenylamino)benzaldehyde and 2,4-dimethylpyrrole were reacted in the presence of TFA followed by DDQ to obtain the corresponding dipyrromethene. This was subsequently converted into BF_2 -chelated dipyrromethene derivative by the reaction BF_3 diethyletherate. This was subsequently converted into BF_2 -chelated dipyrromethane derivative by the reaction BF_3 etherate. This compound was crystallized in CH_2Cl_2 for X-ray diffraction studies. In a separate experiment, a free-base porphyrin derivative was synthesized by the reaction of 3,4-dimethoxybenzaldehyde, *p*-tolualdehyde, and pyrrole in propionic acid followed by demethylation using BBr_3 at $-78^\circ C$.

Metallation of porphyrin using zinc acetate followed by chromatographic separation yielded **1b**. Next, compounds **1a** and **1b** were reacted in the presence of $AlCl_3$ to couple the BDP segment to porphyrin resulting in triad **1**. The phenylimidazole-functionalized fulleropyrrolidine and pyridine-functionalized naphthalenediimide were carried out according literature methods.^[24] The newly synthesized compounds were fully characterized by 1H NMR spectroscopy, MALDI-MS, X-ray analysis for **1a**, electrochemical and other spectroscopic methods as described in the Experimental Section.

The X-ray structure of TPA-BDP dyad, **1a** is shown in Figure 2. The molecule crystallized in the triclinic crystal system.^[22] The distance between boron of BDP and nitrogen of TPA is 8.71 Å, whereas the connecting phenyl ring of the two entities is positioned at 71.8° . The crystal packing diagram (Figure S1), atomic coordinates (Table S1), bond lengths and angles (Tables S2–S4) are given in the Supporting Information.

Optical absorption and emission studies: Figure 3 shows the absorption spectrum of the triad **1** in *o*-dichlorobenzene (DCB). With the help of control compounds Tolyl-BDP and dyad **1a**, it has been possible to assign the absorption peaks corresponding to different entities of the triad. The ZnP bands are located at 427, 554; and 595 nm, whereas the BDP had strong absorbance at 510 nm at which the ZnP absorption is negligible. The TPA entity revealed absorption at 310 nm, overlapped with the UV-bands of ZnP. The negligible absorbance of ZnP in the 510 nm region has given us an opportunity to selectively excite the BDP entity and probe photochemical events.

Figure 4 shows the fluorescence spectrum of **1** under different excitation wavelengths. When excited at 550 nm corresponding to ZnP visible band absorption, two emission bands at 605 and 650 nm were observed. Excitation at 510 nm corresponding to BDP absorption revealed peaks at



Scheme 1. Synthetic methodology adopted for the preparation of TPA-BDP-ZnP triad, **1** in the present study.

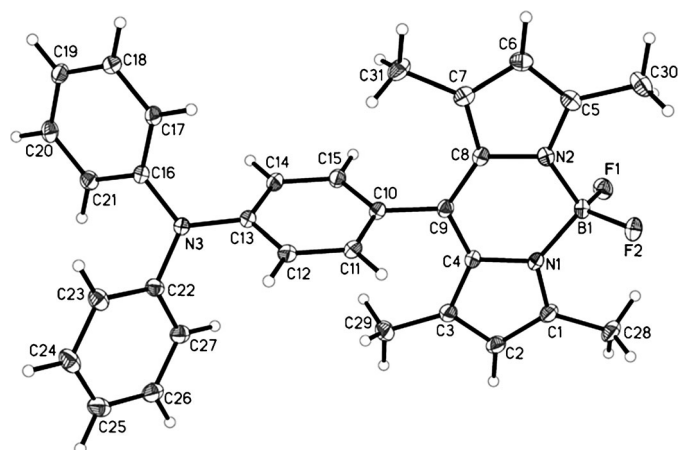


Figure 2. Projection diagram of the TPA-BDP dyad, **1a** with 50% thermal ellipsoids. Disordered part of the molecule (C22A...C27A) is omitted for clarity.

520 nm corresponding to BDP emission and ZnP emission peaks at longer wavelengths. Control experiment performed using pristine TPA-BDP, **1a** revealed BDP peak of much higher intensity (4.5 times larger) and little or no emission

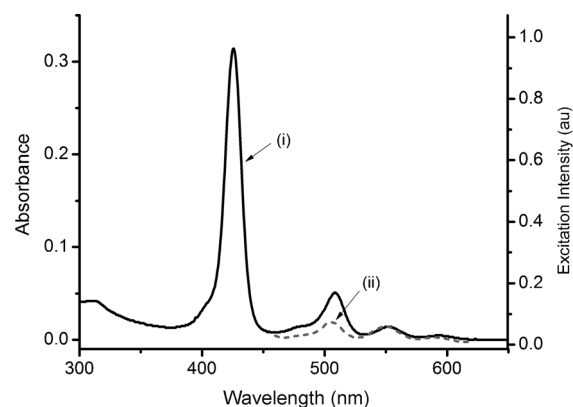


Figure 3. (i) Absorption spectrum and (ii) excitation spectrum of **1** in DCB. For recording excitation spectrum, emission monochromator was set to 650 nm corresponding to ZnP emission, and excitation was scanned.

of ZnP at the same excitation conditions. The diminished intensity of BDP emission and appearance of ZnP emission suggest occurrence excited energy transfer.^[23] To secure additional proof for energy transfer, excitation spectrum was recorded by setting the emission monochromator to por-

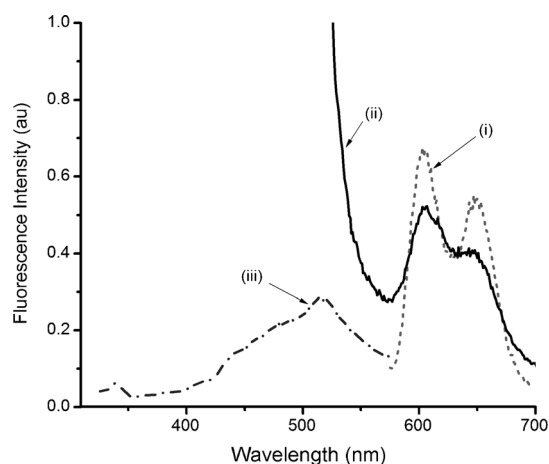


Figure 4. Fluorescence spectra of **1** in DCB under different excitation wavelengths; (i) 550 nm corresponding to ZnP absorption, (ii) 510 nm corresponding to BDP absorption and (iii) 310 nm corresponding to TPA absorbance.

phyrin emission. As shown in Figure 4, the spectrum revealed peaks not only of ZnP but also of BDP confirming the occurrence of energy transfer.^[23] The absorption and excitation spectra were normalized to the 550 nm peak to compare the intensity of the BDP band at 510 nm. Such comparison in Figure 3 gave an estimation of efficiency of energy transfer to be about 50% because the BDP band of the excitation spectrum was about half as much as that observed in the absorption spectrum of **1**. The lower efficiency of excitation transfer compared with an earlier reported BDP-ZnP dyad could be due to competing electron transfer from singlet excited BDP to TPA entity (see below).^[6f] When the TPA entity of **1** was excited at 307 nm, broad emission in the region of 440–550 nm with a peak at 520 nm corresponding to BDP emission was observed. However, peak intensity of ZnP at 427 or 550 nm was less. Under similar experimental conditions, the emission spectrum of the control compound, TPA-BDP revealed absence of ZnP emission. This suggests energy transfer, from excited TPA to the neighbor BDP and not distantly located ZnP. The broad emission in the 440 nm could be due to weak emission of TPA, and energy transfer from singlet excited BDP (product of initial energy transfer) to ZnP. These spectral observations reveal sequential energy transfer, although not very efficient, from excited TPA to BDP to ZnP when TPA was excited and BDP to ZnP when BDP was excited, as shown in Figure 1.

Supramolecular tetrad formation through axial coordination of electron acceptors:

Having established photoinduced sequential energy transfer in the TPA-BDP-ZnP triad, next we focused on incorporating an electron acceptor moiety by using the well-established metal–ligand axial coordination approach.^[7a,21] In the present study, we have employed two types of electron acceptors, fullerene appended with phenylimidazole, C_{60} Im and naphthalenediimide functionalized with a pyridine entity, NDIPy.^[24] Figure 5a shows the absorption spectral changes during titration of C_{60} Im to a solu-

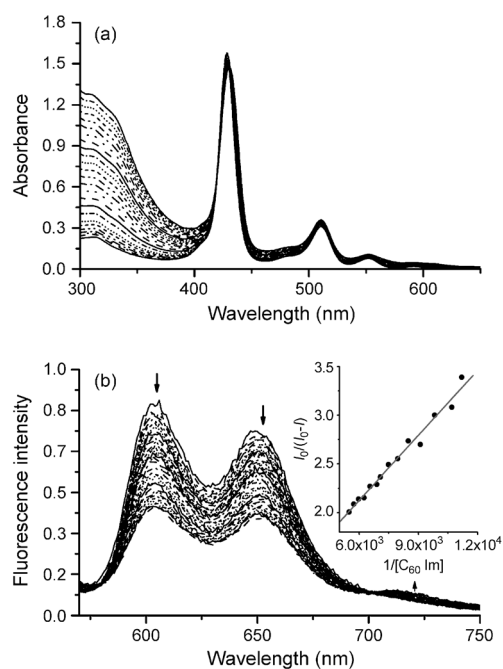


Figure 5. (a) Absorption and (b) fluorescence spectral changes of **1** during increased addition of C_{60} Im to form the tetrad. Figure 5b inset shows Benesi–Hildebrand plot constructed to evaluate the binding constant.

tion of **1**. The optical absorption bands of ZnP of the triad revealed spectral changes characteristic of axial ligation without causing significant spectral shifts in the BDP absorption peak at 510 nm; that is, the porphyrin Soret at 427 nm revealed a red shift of 5 nm and appeared at 432 nm. An isosbestic point was also observed at 419 nm indicating the presence of only one equilibrium process. The ZnP emission was also found to be quenched during binding of C_{60} Im to **1** as shown in Figure 5b. A new emission band at 713 nm was observed and independent experiments confirmed that this peak is due to fulleropyrrolidine at the excitation maxima and not as a result of energy transfer. Using the quenching data, the binding constant, K evaluated using Benesi–Hildebrand method^[25] was found to be $3.6 \times 10^3 \text{ M}^{-1}$. The magnitude of this value was nearly four times smaller compared to C_{60} Im binding to tetraphenylporphyrinato zinc(II) without BDP and TPA entities, perhaps due to the electronic effects caused by these entities. A plot of mole ratio method confirmed 1:1 stoichiometry for the newly assembled complex.

Similar spectral changes were made during NDIPy binding to **1**, that is, binding of pyridine entity of NDIPy to ZnP associated absorption changes, fluorescence quenching and 1:1 molecular stoichiometry (see the Supporting Information, Figure S3 for spectral changes). The evaluated binding constant from optical absorption spectral studies was found to be $K = 4.57 \times 10^3 \text{ M}^{-1}$, which is comparable to that obtained for C_{60} Im binding to **1**.

Molecular orbital calculations using B3LYP/3-21G(*)^[26,27] were performed to visualize the geometry and electronic

structure of $C_{60}Im:1$ and $NDIpy:1$ tetrads. Figure 6a and b show the optimized structures of the two tetrads. In the optimized structures, the BDP and ZnP macrocycles in almost

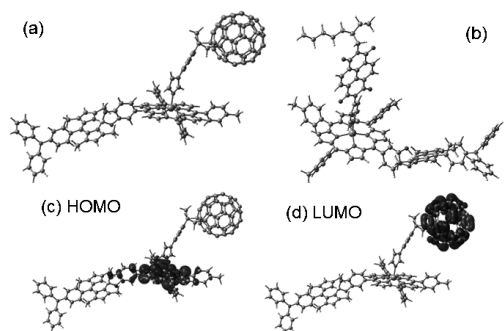


Figure 6. B3LYP/3-21G(*) optimized structures of (a) $C_{60}Im:ZnP-BDP-TPA$ and (b) $NDIpy:ZnP-BDP-TPA$ supramolecular tetrads. The frontier HOMO and LUMO orbitals of multi-modular $C_{60}Im:ZnP-BDP-TPA$ supramolecular tetrad are shown in (c) and (d).

the same plane, and the TPA and BDP macrocycles geometry were similar to the X-ray structure discussed in the previous section. The $C_{60}Im:ZnP$ segment was also close to earlier reported X-ray structure^[28a] with a center-to-center distance of 13.1 Å. In the case of $NDIpy:1$ tetrad, similar structure was observed with a center-to-center distance of 9.86 Å between the ZnP and $NDIpy$ entities.^[28b] An important observation is the placement of the acceptor entity away from the BDP macrocycle in the optimized structures, further X-ray structure may be needed to validate such structures. As expected, the first two HOMOs were localized on the ZnP entity with some contributions on the catechol-boron segment; however, the first two LUMOs were fully located on the electron acceptor entities, as shown for $C_{60}Im:1$ in Figure 6c and d for the first HOMO and LUMO.

Electrochemical studies and energy states: Cyclic voltammetry (CV) experiments were performed to evaluate the redox potentials. The redox potentials of individual entities were determined by performing experiments involving the control compounds, the dyads and the monomers (see Figure S2 in Supporting Information). Dyad, **1a** revealed a reversible reduction located at -1.75 V versus Fc/Fc^+ corresponding to the reduction of the BDP entity. There was also a multi-electron anodic process at $E_{pa}=0.89$ V due to the oxidation of TPA and BDP entities. Another dyad BDP-ZnP without the TPA entity was synthesized.^[32a] The CV of this dyad revealed two reductions at -1.70 and -2.01 V versus Fc/Fc^+ corresponding to the reductions of BDP and ZnP entities, respectively. On the anodic side, two reversible oxidations at 0.20 and 0.56 V versus Fc/Fc^+ were observed corresponding to first and second oxidations of the ZnP entity. The CV of the triad, **1** revealed redox processes corresponding to all three entities; that is, BDP reduction at -1.70 V, ZnP first reduction at -2.00 V, first two oxidations of ZnP at 0.18 and 0.49 V, and an irreversible oxidation involving both TPA

and BDP at $E_{pa}=0.81$ V versus Fc/Fc^+ , respectively, were observed. These potentials were slightly different from the control compounds indicating some intramolecular interactions between the entities.

Figure 7 shows CV of **1** on increasing addition of $C_{60}Im$ in DCB containing 0.1 M $(TBA)ClO_4$. In addition to the redox peaks of **1**, redox processes of $C_{60}Im$ were also observed.

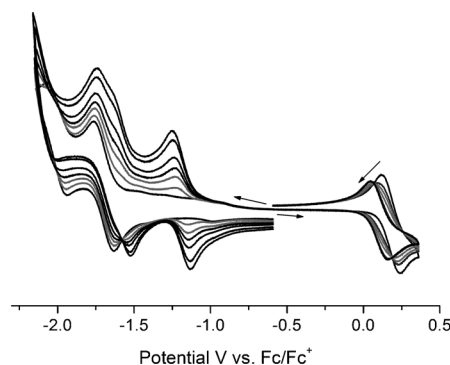


Figure 7. Cyclic voltammograms of triad, **1** on increasing addition of $C_{60}Im$ (0.15 equiv each addition) in DCB, 0.1 M $(TBA)ClO_4$. Scan rate = 100 mV s⁻¹.

The first reduction of $C_{60}Im$ was located at -1.19 V versus Fc/Fc^+ , whereas the second one at -1.58 V was close to the first reduction of BDP entity. Interestingly, the first oxidation process of ZnP located at 0.20 V revealed a cathodic shift of about 90 mV and appeared at 0.11 V due to imidazole entity of $C_{60}Im$ binding to ZnP.^[29] The first reduction of $NDIpy$ was located at -1.17 V and upon binding to ZnP, the potential shifts were not significantly different.^[24]

Free-energy calculations for charge-recombination (ΔG_{CR}) and charge-separation (ΔG_{CS}) processes were performed according to Equations (1) and (2) based on the Weller approach:^[30]

$$-\Delta G_{CR} = e(E_{ox} - E_{red}) + \Delta G_s \quad (1)$$

$$-\Delta G_{CS} = \Delta E_{0-0} - (-\Delta G_{CR}) \quad (2)$$

in which ΔE_{00} and ΔG_s correspond to the energy of $^1ZnP^*$ and electrostatic energy, respectively. The E_{ox} and E_{red} represent the oxidation potential of the electron donor (ZnP) and the reduction potential of the electron acceptor ($C_{60}Im$ or $NDIpy$), respectively. ΔG_s refers to the static energy, calculated by using the "Dielectric continuum model" according to Equation (3):

$$-\Delta G_s = -(e^2/(4\pi\epsilon_0))[(1/(2R_+) + 1/(2R_-)) - (1/R_{CC})]/\epsilon_s - (1/(2R_+) + 1/(2R_-))/\epsilon_R \quad (3)$$

in which R_+ and R_- are radii of the radical cation and radical anion, respectively; R_{CC} represents the center-center distances between ZnP and $C_{60}Im$ and $NDIpy$, which were

evaluated from the optimized structure. The symbols ϵ_R and ϵ_S refer to solvent dielectric constants for electrochemistry and photophysical measurements, respectively.

The ΔG_{CR} is determined to be -1.40 and -1.44 eV, respectively, for fullerene and naphthalenediimide acceptors in DCB.^[30] The ΔG_{CS} is estimated to be -0.68 and -0.64 eV, respectively, for fullerene and naphthalenediimide acceptors with respect to ΔG_{CR} value and energy of singlet excited state of ZnP (2.08 eV) (see Table 1 below). It should be

Table 1. Redox potentials and free-energy changes for charge-separation (ΔG_{CS}) from the singlet excited state of the ZnP and charge-recombination (ΔG_{CR}) for the investigated compounds in *o*-dichlorobenzene and toluene.

Compound	1st Ox ^[a]	1st Red ^[a]	$-\Delta G_{CS}$ ^[b]	$-\Delta G_{CR}$ ^[c]
1a	0.89	-1.75	–	–
BDP-ZnP	0.20	-1.70	$0.08^{[d]}$	$2.00^{[d]}$
1	0.18	-1.70	$0.10^{[d]}$	$1.98^{[d]}$
C ₆₀ Im: 1	0.11	-1.19	$0.68^{[d]}$ $0.38^{[e]}$	$1.40^{[d]}$ $1.70^{[e]}$
NDIpy: 1	0.17	-1.17	$0.64^{[d]}$ $0.34^{[e]}$	$1.44^{[d]}$ $1.74^{[e]}$

[a] Additional redox processes are observed, see text for details; [b] from Equation (2); [c] from Equation (1); [d] in *o*-dichlorobenzene; [e] in toluene.

noted, however, the $-\Delta G_{CS}$ and $-\Delta G_{CR}$ values determined from the redox potentials in Figure 7 provide the values in the presence of 0.10 M (TBA)ClO₄, which stabilizes the CS state by the electrostatic interaction with (TBA)ClO₄. However, by taking into consideration that the Weller model in nonpolar toluene is likely to be oversimplified, it is possible to consider the energy of the charge-separated state of C₆₀Im:**1** (1.70 eV) and NDIpy:**1** (1.74 eV) tetrads in toluene as higher than that of ³ZnP* (1.56 eV).

Transient absorption studies: Femtosecond and nanosecond transient spectral measurements were performed in toluene to monitor the kinetics of energy and electron transfer events in the studied polyads. The femtosecond transient absorption spectra of the triad **1** (Figure 8) revealed the instantaneous formation of the BDP singlet-excited state features. Here, the transient absorption spectra exhibited the bleaching in the visible region with a maximum at 510 nm.^[31] With time, the BDP singlet excited diminished in intensity with concomitant increase of the ZnP absorption in the visible region providing the direct evidence of excitation transfer from the singlet excited BDP to ZnP.^[32] The rate constant of energy transfer (k_{ENT}) from ¹BDP* to the ZnP moiety was determined by exponential fitting of the decay of ¹BDP* and the rise of ¹ZnP* to be $1.0 \times 10^{12} \text{ s}^{-1}$ confirming occurrence of fast and efficient energy transfer from ¹BDP* to ZnP.

The transient absorption spectral changes were distinctly different when either of the electron acceptor was bound to **1**, that is, spectral features corresponding to charge separation was observed. Figure 9 shows spectral changes recorded during C₆₀Im binding to **1** in non-polar toluene.^[33,34] Clear transient bands in the 600 nm range corresponding to the

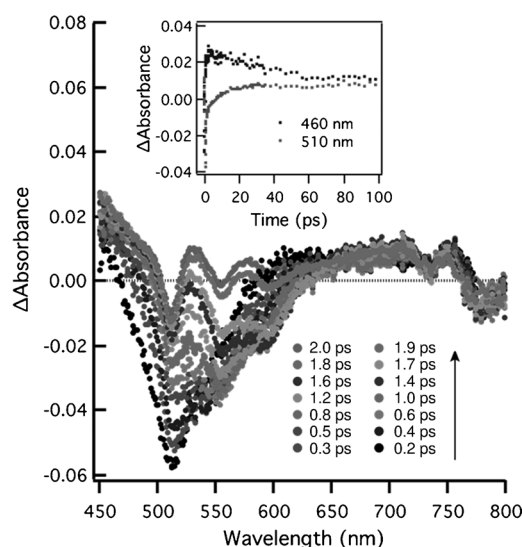


Figure 8. Femtosecond transient absorption spectra obtained by 460 nm laser excitation of **1** in deaerated toluene. Inset: Decay time profiles of the ¹BDP* at 510 nm and the ¹ZnP* at 460 nm.

formation of ZnP⁺ and around 1000 nm corresponding to the formation C₆₀Im[−] were observed. No features corresponding to BDP[−] or TPA⁺ were there suggesting that these entities in the supramolecular assembly are involved only in excitation transfer and not electron transfer. The rates of charge separation, k_{CS} and charge recombination, k_{CR} were evaluated by monitoring the rise and decay of the C₆₀Im[−] as shown in the inset Figure 9. The calculated k_{CS} and k_{CR} were found to be $5.00 \times 10^9 \text{ s}^{-1}$ and $2.10 \times 10^8 \text{ s}^{-1}$, respectively, revealing fairly fast electron-transfer events.

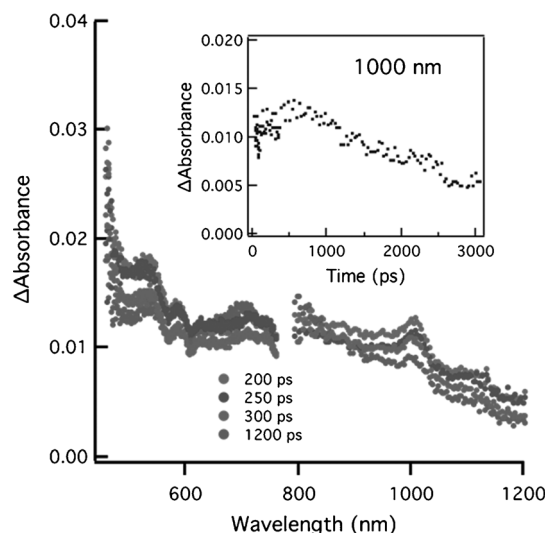


Figure 9. Femtosecond transient absorption spectra obtained by 460 nm laser excitation of C₆₀Im:**1** in deaerated toluene. Inset: shows the rise-decay profiles of C₆₀[−] at 1000 nm.

Figure 10 shows the transient spectra at different time intervals for NDIpy:**1** complex in deaerated toluene. Charac-

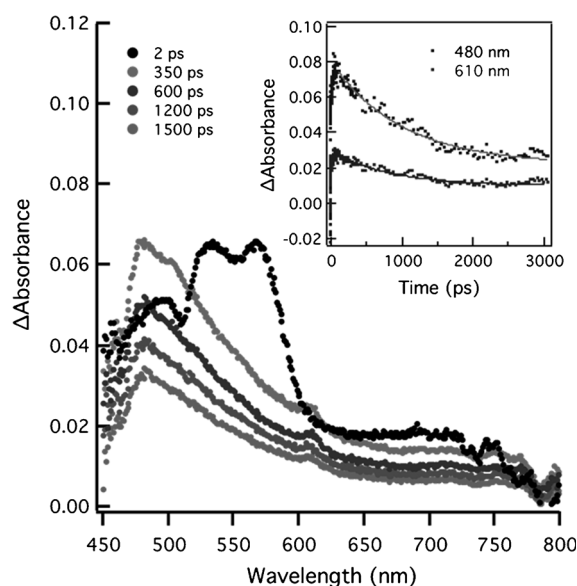


Figure 10. Femtosecond transient absorption spectra obtained by 460 nm laser excitation of NDIPy:1 in deaerated toluene. Figure inset shows the time profiles of the 480 and 610 nm bands.

teristic features of NDIPy^{•-} around 490 nm and ZnP^{•+} around 600 nm confirming the formation of radical pair ion were observed.^[24] By monitoring the rise and decay of these bands (see Figure 10, inset), the k_{CS} and k_{CR} were evaluated and these were found to be 3.47×10^{10} and $8.40 \times 10^8 \text{ s}^{-1}$, respectively. These values are slightly larger than that observed for C₆₀Im:1 that could be rationalized for the fairly rigid two-dimensional electron acceptor naphthalenediimide as compared to the three-dimensional electron acceptor fullerene. Compared with that of NDIPy:1, the slightly slower of CS and CR processes of C₆₀Im:1 may also be rationalized by the longer distance-to-distance between the C₆₀Im and ZnP.

Further nanosecond transient spectra for the examined compounds in deaerated toluene were measured, as shown in Figure 11 and in the Supporting Information S4–S6. All of the compounds, that is, dyad **1b**, triad **1**, and the supramolecular tetrads C₆₀Im:1 and NDIPy:1 were excited by using 430 nm, which selectively excited the ZnP entity. The transient absorption spectra of C₆₀Im:1 in Figure 11 exhibited the transient bands of the triplet ZnP at 480 nm, in addition to broad absorption bands in the visible region. The characteristic absorption bands of the ZnP radical cation and C₆₀ radical anion were not observed in the visible and NIR region. The observation of the ZnP triplet together with no observation of the CS state is in a good agreement with the finding that the CS energy is higher than the triplet energy of ZnP (1.56 eV) (see above).^[21] The ZnP triplet decayed with a rate constant of $4.00 \times 10^4 \text{ s}^{-1}$. Similar observations were made in the case of 1:NDIPy (the Supporting Information, Figure S7).

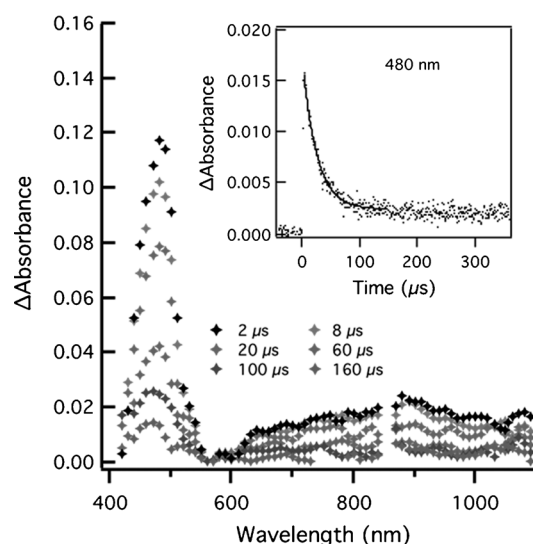


Figure 11. Nanosecond transient spectra of C₆₀Im:1 in deaerated toluene; λ_{ex} = 430 nm. Inset shows the decay profile of the 480 nm band.

Conclusion

Multi-modular donor–acceptor complexes have been assembled to probe sequential energy- and electron-transfer processes by careful selection of energy-imparting entities coupled to well-known zinc porphyrin–fullerene or zinc porphyrin–naphthalenediimide donor–acceptor conjugates. The newly synthesized triad for this purpose featured triphenylamine, boron dipyrin and zinc porphyrin entities, and was characterized by various spectral and electrochemical methods, including X-ray analysis of the dyad, **1a**. Excitation of the energy-imparting triphenylamine or BDP entities resulted excitation transfer; femtosecond transient studies revealed such a process is extremely fast and occurs in the order of sub-ps. Panchromatic energy-harvesting was observed in this molecule. The structural integrity of the donor–acceptor polyad obtained by axial coordination of fullerene or naphthalenediimide was established from computational, spectral, and electrochemical studies. The presence of an electron acceptor in the polyad promoted electron transfer, which resulted in a charge separated species; a result fully supported by free-energy calculations. The presence of either a fullerene or naphthalenediimide entity revealed that fast-forward electron-transfer and relatively slow back electron-transfer occurs in these new polyads, which highlights their significance as artificial antenna-reaction center models of photosynthesis.

Experimental Section

Chemicals: All of the reagents used in the syntheses, and *o*-dichlorobenzene (in sure seal bottle under nitrogen) were obtained from Aldrich Chemicals (Milwaukee, WI). Tetra-*n*-butylammonium perchlorate, (TBA)ClO₄ was obtained from Fluka Chemicals. All the chromatographic materials and solvents were procured from Fisher Scientific and were

used as received. All the chromatographic materials and solvents were procured from Fisher Scientific and were used as received.

Synthesis of meso-triphenylamino-difluoroboron dipyrin, 1a:^[35] To a mixture of 4-(diphenylamino)benzaldehyde (3.39 g, 12.4 mmol) and 2,4-dimethylpyrrole (2.16 mL, 21.1 mmol) in CH₂Cl₂ (800 mL), trifluoroacetic acid (0.19 mL, 2.47 mmol) was added. The reaction mixture was stirred at room temperature under argon. After 1.5 h the resulting solution was washed with 0.1 M NaOH (200 mL) and then water (200 mL). The organic layer was dried over anhydrous Na₂SO₄ and evaporated under reduced pressure. The residue was dissolved in toluene (50 mL) and with stirring *p*-chloranil (2.73 g, 11.1 mmol) was added. After 10 min Et₃N (8 mL) was added followed by BF₃·Et₂O (7 mL). The mixture was stirred for 1.5 h and then poured into water. The organic layer was extracted and dried over anhydrous Na₂SO₄ and evaporated under reduced pressure. The crude product was purified using column chromatography. ¹H NMR (300 MHz, CDCl₃): δ = 7.21–7.39 (m, 6H), 7.0–7.12 (m, 8H), 6.0 (s, 2H), 2.59 (s, 6H), 1.6 ppm (s, 6H).

Synthesis of 5-[2,2'-(3,4-dimethoxyphenyl)]-10,15,20-tritolyl-porphyrin: This compound was synthesized by treating 3,4-dimethoxybenzaldehyde (1.55 g, 9.33 mmol), tolaldehyde (3.31 mL, 28 mmol), and pyrrole (2.6 mL, 37.26 mmol) in propionic acid (200 mL). The reaction mixture was refluxed for 2 h and then the solvent was evaporated under reduced pressure. The crude product was purified on a basic alumina column. ¹H NMR (300 MHz, CDCl₃): δ = 8.94–8.86 (m, 8H), 8.14–8.08 (m, 6H), 7.81–7.80 (m, 1H), 7.79–7.74 (m, 1H), 7.58–7.52 (m, 6H), 7.24–7.20 (m, 1H), 4.20 (s, 3H), 4.0 (s, 3H), –2.69 ppm (brs, 2H).

Synthesis of 5-[2,2'-(3,4-dihydroxyphenyl)]-10,15,20-tritolyl-porphyrin: This compound was synthesized according to the reported procedure with few modifications.^[36] BBr₃ (9 mL, 1 M in CH₂Cl₂) was dropwise added to a solution of 3,4-dimethoxyphenyl porphyrin (1.0 mmol) in CH₂Cl₂ at –78 °C. The solution was maintained at this temperature until the addition was completed and stirred at room temperature for 12 h. Then the mixture was brought to below 5 °C and cold water (100 mL) was added followed by addition of saturated sodium bicarbonate. After stirring for 1 h at room temperature, the organic layer was separated using CH₂Cl₂ and dried over anhydrous Na₂SO₄. The solvent was evaporated and the crude product was purified on silica column. ¹H NMR (300 MHz, CDCl₃): δ = 8.95–8.86 (m, 8H), 8.14–8.08 (m, 6H), 7.81–7.80 (m, 1H), 7.79–7.74 (m, 1H), 7.58–7.52 (m, 6H), 7.24–7.20 (m, 1H), 2.70 (s, 9H), –2.69 ppm (brs, 2H).

Synthesis of 5-[2,2'-(3,4-dihydroxyphenyl)]-10,15,20-tritolyl porphyrinato-zinc(II): An excess of zinc acetate dihydrate (50 equiv) in methanol was added to free base porphyrin (0.0125 mmol) from the previous step dissolved in CHCl₃ (30 mL). The course of the reaction was monitored spectroscopically until the reaction was complete. After the workup, the organic layer was evaporated and the crude was purified on silica gel column. At the end of the reaction (1 h), the solvent was evaporated and the product was purified on silica gel column. ¹H NMR (300 MHz, CDCl₃): δ = 8.95–8.86 (m, 8H), 8.14–8.08 (m, 6H), 7.81–7.80 (m, 1H), 7.79–7.74 (m, 1H), 7.58–7.52 (m, 6H), 7.24–7.20 (m, 1H), 2.70 ppm (s, 9H).

Synthesis of TPA-BDP-ZnP triad, 1: Compound 1a (0.183 mmol) was dissolved in dry CH₂Cl₂ (20 mL) and stirred under argon for 10 min. Then, AlCl₃ (36.5 mg, 0.274 mmol) was added and stirred further 15 min before addition of 3,4-dihydroxyphenylporphyrinatozinc, 1b (206.11 mg, 0.274 mmol). The mixture was stirred for 30 min and the solvent was evaporated under reduced pressure. The crude product was purified using a deactivated basic alumina column to give desired compound. ¹H NMR (300 MHz, CDCl₃): δ = 9.12–8.92 (m, 8H), 8.20–8.18 (m, 6H), 7.81–7.80 (m, 1H), 7.78–7.74 (m, 1H), 7.61–7.52 (m, 6H), 7.39–7.120 (m, 15H), 6.10 (s, 2H), 2.78 (s, 9H), 2.59 (s, 6H), 1.71 ppm (s, 6H); MALDI-MS: *m/z*: calcd for C₇₈H₆₀N₇O₂BZn: 1203.11 [M⁺]; found: 1202.79.

Instruments: The UV/Vis spectral measurements were carried out with a Shimadzu Model 2550 double monochromator UV/Vis spectrophotometer. The fluorescence emission was monitored by using a Varian Eclipse spectrometer. A right angle detection method was used. The ¹H NMR studies were carried out on a Bruker 300 Hz spectrometer. Tetramethylsilane (TMS) was used as an internal standard.

Crystal structure determination for compound 1a was carried out using a Bruker SMATR APEX2 CCD-based X-ray diffractometer equipped with a low temperature device and Mo-target X-ray tube (wavelength = 0.71073 Å). Measurements were taken at 100(2) K.

Cyclic voltammograms were recorded on an EG&G PARSTAT electrochemical analyzer using a three electrode system. A platinum button electrode was used as the working electrode. A platinum wire served as the counter electrode and an Ag/AgCl electrode was used as the reference electrode. Ferrocene/ferrocenium redox couple was used as an internal standard. All the solutions were purged prior to electrochemical and spectral measurements using argon gas. MALDI-TOF spectrum of the ZnP-BDP-TPA triad was recorded in dichloromethane with an Applied Biosystems Voyager-DE-STR using dithranol as a matrix (Supporting Information, Figure S7). The computational calculations were performed by DFT B3LYP/3–21G* methods by using the Gaussian 09 software package^[26] on high speed PCs. The frontier HOMO and LUMO were generated by using GaussView software.

Laser flash photolysis: The studied compounds were excited by a Panther OPO pumped by Nd:YAG laser (Continuum, SLII-10, 4–6 ns fwhm) with the powers of 1.5 and 3.0 mJ per pulse. The transient absorption measurements were performed using a continuous xenon lamp (150 W) and an InGaAs-PIN photodiode (Hamamatsu 2949) as a probe light and a detector, respectively. The output from the photodiodes and a photomultiplier tube was recorded with a digitizing oscilloscope (Tektronix, TDS3032, 300 MHz). Femtosecond transient absorption spectroscopy experiments were conducted using an ultrafast source: Integra-C (Quantronix Corp.), an optical parametric amplifier: TOPAS (Light Conversion Ltd.) and a commercially available optical detection system: Helios provided by Ultrafast Systems LLC. The source for the pump and probe pulses were derived from the fundamental output of Integra-C (780 nm, 2 mJ per pulse and fwhm = 130 fs) at a repetition rate of 1 kHz. 75 % of the fundamental output of the laser was introduced into TOPAS, which has optical frequency mixers resulting in tunable range from 285 nm to 1660 nm, whereas the rest of the output was used for white light generation. Typically, 2500 excitation pulses were averaged for 5 seconds to obtain the transient spectrum at a set delay time. Kinetic traces at appropriate wavelengths were assembled from the time-resolved spectral data. All measurements were conducted at 298 K. The transient spectra were recorded using fresh solutions in each laser excitation.

Acknowledgements

This work was supported by National Science Foundation (Grant No. CHE1110942 to F.D.), and the Global COE (center of excellence) program “Global Education and Research Center for Bio-Environmental Chemistry” of Osaka University from Ministry of Education, Culture, Sports, Science and Technology, Japan, and KOSEF/MEST through the WCU project (R31–2008–000–10010–0) from Korea.

- [1] a) J. Deisenhofer, O. Epp, K. Miki, R. Huber, H. Michel, *J. Mol. Biol.* **1984**, 180, 385; b) *The Photosynthetic Reaction Center* (Eds.: J. Deisenhofer, J. R. Norris), Academic Press, San Diego, CA, **1993**; c) C. Kirmaier, D. Holton in *The Photosynthetic Reaction Center, Vol II* (Eds.: J. Deisenhofer, J. R. Norris), Academic Press, San Diego, CA, **1993**, pp. 49–70; d) *Molecular Mechanisms of Photosynthesis* (Ed.: R. E. Blankenship), Blackwell Sciences, Oxford, **2002**; e) *Handbook of Photosynthesis*, 2nd Ed. (Ed.: M. Pessarakli), CRC Press LLC, Boca Raton, FL, **2005**; f) *Photosynthetic Light Harvesting* (Eds.: R. Cogdell, C. Mullineaux), Springer, Dordrecht, Netherland, **2008**.
- [2] a) M. R. Wasielewski, *Chem. Rev.* **1992**, 92, 435; b) D. Gust, T. A. Moore in *The Porphyrin Handbook, Vol 8* (Eds.: K. M. Kadish, K. M. Smith, R. Guilard), Academic Press, Burlington, MA, **2000**, pp. 153–190; c) D. Gust, T. A. Moore, A. L. Moore, *Acc. Chem. Res.* **2001**, 34, 40; d) D. Gust, T. A. Moore, A. L. Moore, *Acc. Chem. Res.*

- 2009, 42, 1890; e) M. R. Wasielewski, *Acc. Chem. Res.* **2009**, 42, 1910.
- [3] a) A. Harriman, J. P. Sauvage, *Chem. Soc. Rev.* **1996**, 25, 41; b) V. Balzani, A. Juris, M. Venturi, S. Campagna, S. Serroni, *Chem. Rev.* **1996**, 96, 759; c) M. J. Blanco, M. C. Jiménez, J. C. Chambron, V. Heitz, M. Linke, J. P. Sauvage, *Chem. Soc. Rev.* **1999**, 28, 293; d) *Electron Transfer in Chemistry* (Ed.: V. Balzani), Wiley-VCH, Weinheim, Germany, **2001**; e) N. Armaroli, V. Balzani, *Angew. Chem.* **2007**, 119, 52; *Angew. Chem. Int. Ed.* **2007**, 46, 52.
- [4] a) H. Imahori, S. Fukuzumi, *Adv. Funct. Mater.* **2004**, 14, 525; b) I. Bouamaied, T. Coskun, E. Stulz, *Struct. Bond.* **2006**, 121, 1; c) S. Fukuzumi, *Phys. Chem. Chem. Phys.* **2008**, 10, 2283; d) D. I. Schuster, K. Li, D. M. Guldi, *C. R. Chim.* **2006**, 9, 892; e) J. N. Clifford, G. Accorsi, F. Cardinali, J. F. Nierengarten, N. Armaroli, *C. R. Chim.* **2006**, 9, 1005; f) G. de La Torre, C. G. Claessens, T. Torres, *Chem. Commun.* **2007**, 2000; g) S. Fukuzumi, *Pure Appl. Chem.* **2007**, 79, 981; h) S. Fukuzumi, T. Kojima, *J. Mater. Chem.* **2008**, 18, 1427; i) S. Fukuzumi, *Bull. Chem. Soc. Jpn.* **2006**, 79, 177.
- [5] a) D. M. Guldi, *Chem. Commun.* **2000**, 321; b) L. Sánchez, M. Nazario, D. M. Guldi, *Angew. Chem.* **2005**, 117, 5508; *Angew. Chem. Int. Ed.* **2005**, 44, 5374; c) A. Mateo-Alonso, D. M. Guldi, F. Paolucci, M. Prato, *Angew. Chem.* **2007**, 119, 8266; *Angew. Chem. Int. Ed.* **2007**, 46, 8120; d) D. M. Guldi, *Phys. Chem. Chem. Phys.* **2007**, 9, 1400; e) V. Sgobba, D. M. Guldi, *Chem. Soc. Rev.* **2009**, 38, 165.
- [6] a) J. S. Sessler, B. Wang, S. L. Springs, C. T. Brown in *Comprehensive Supramolecular Chemistry* (Eds.: J. L. Atwood, J. E. D. Davies, D. D. MacNicol, F. Vogtle), Pergamon, New York, **1996**, Chapter 9; b) J. L. Sessler, C. M. Lawrence, J. Jayawickramarajah, *Chem. Soc. Rev.* **2007**, 36, 314; c) J.-Y. Liu, M. E. El-Khouly, S. Fukuzumi, D. K. P. Ng, *Chem. Eur. J.* **2011**, 17, 1605; d) M. E. El-Khouly, D. K. Ju, K.-Y. Kay, F. D'Souza, S. Fukuzumi, *Chem. Eur. J.* **2010**, 16, 6193; e) F. D'Souza, C. A. Wijesinghe, M. E. El-Khouly, J. Hudson, M. Niemi, H. Lemmetyinen, N. V. Tkachenko, M. E. Zandler, S. Fukuzumi, *Phys. Chem. Chem. Phys.* **2011**, 13, 18168; f) F. D'Souza, P. M. Smith, M. E. Zandler, A. L. McCarty, M. Itou, Y. Araki, O. Ito, *J. Am. Chem. Soc.* **2004**, 126, 7898.
- [7] a) F. D'Souza, O. Ito, *Coord. Chem. Rev.* **2005**, 249, 1410; b) R. Chitta, F. D'Souza, *J. Mater. Chem.* **2008**, 18, 1440; c) F. D'Souza, O. Ito in *Handbook of Organic Electronics and Photonics, Vol 1* (Ed.: H. S. Nalwa), American Scientific Publishers, California, **2008**, Chapter 13, pp. 485–521; d) F. D'Souza, O. Ito, In *Handbook of Porphyrin Science* (Eds. K. M. Kadish, R. Guilard, K. M. Smith), World Science Publishers, **2010**, Vol. 1, Chapter 4, pp. 307–437; e) F. D'Souza, A. S. D. Sandanayaka, O. Ito, *J. Phys. Chem. Lett.* **2010**, 1, 2586; f) F. D'Souza, O. Ito, *Chem. Soc. Rev.* **2012**, 41, 86.
- [8] a) S. Fukuzumi, T. Honda, K. Ohkubo, T. Kojima, *Dalton Trans.* **2009**, 3880; b) S. Fukuzumi, K. Ohkubo, *J. Mater. Chem.* **2012**, 22, 4575; c) S. Fukuzumi, K. Ohkubo, F. D'Souza, J. L. Sessler, *Chem. Commun.* **2012**, 48, 9801.
- [9] a) *Energy Harvesting Materials* (Ed.: D. L. Andrews), World Scientific, Singapore, **2005**; b) S. Günes, H. Neugebauer, N. S. Sariciftci, *Chem. Rev.* **2007**, 107, 1324; c) P. V. Kamat, *J. Phys. Chem. C* **2007**, 111, 2834; d) B. C. Thompson, J. M. J. Frechet, *Angew. Chem.* **2008**, 120, 62; *Angew. Chem. Int. Ed.* **2008**, 47, 58.
- [10] a) T. Hasobe, S. Fukuzumi, P. V. Kamat, *Interface* **2006**, 35, 47; b) T. Hasobe, H. Imahori, P. V. Kamat, T. K. Ahn, D. Kim, T. Hanada, T. Hirakawa, S. Fukuzumi, *J. Am. Chem. Soc.* **2005**, 127, 1216; c) T. Hasobe, K. Saito, P. V. Kamat, V. Troiani, H. Qiu, N. Solladié, T. K. Ahn, K. S. Kim, S. K. Kim, D. Kim, F. D'Souza, S. Fukuzumi, *J. Mater. Chem.* **2007**, 17, 4160; d) D. Hirayama, K. Takimiya, Y. Aso, T. Otsubo, T. Hasobe, H. Yamada, H. Imahori, S. Fukuzumi, Y. Sakata, *J. Am. Chem. Soc.* **2002**, 124, 532; e) F. D'Souza, A. N. Amin, M. E. El-Khouly, N. K. Subbaiyan, M. E. Zandler, S. Fukuzumi, *J. Am. Chem. Soc.* **2012**, 134, 654.
- [11] a) H. Kotani, K. Ohkubo, Y. Takai, S. Fukuzumi, *J. Phys. Chem. B* **2006**, 110, 24047; b) H. Kotani, T. Ono, K. Ohkubo, S. Fukuzumi, *Phys. Chem. Chem. Phys.* **2007**, 9, 1487; c) S. Fukuzumi, *Eur. J. Inorg. Chem.* **2008**, 1351.
- [12] a) S. Fukuzumi, Y. Yamada, T. Suenobu, K. Ohkubo, H. Kotani, *Energy Environ. Sci.* **2011**, 4, 2754; b) H. Kotani, R. Hanazaki, K. Ohkubo, Y. Yamada, S. Fukuzumi, *Chem. Eur. J.* **2011**, 17, 2777; c) Y. Yamada, T. Miyahigashi, H. Kotani, K. Ohkubo, S. Fukuzumi, *Energy Environ. Sci.* **2012**, 5, 6111; d) Y. Yamada, T. Miyahigashi, H. Kotani, K. Ohkubo, S. Fukuzumi, *J. Am. Chem. Soc.* **2011**, 133, 16136.
- [13] H. Sakai, H. Murata, M. Murakami, K. Ohkubo, S. Fukuzumi, *Appl. Phys. Lett.* **2009**, 95, 252901.
- [14] a) H. Kotani, K. Ohkubo, S. Fukuzumi, *J. Am. Chem. Soc.* **2004**, 126, 15999; b) K. Ohkubo, T. Nanjo, S. Fukuzumi, *Catal. Today* **2006**, 117, 356; c) H. Kotani, K. Ohkubo, S. Fukuzumi, *Appl. Catal. B* **2008**, 77, 317; d) K. Ohkubo, K. Mizushima, S. Fukuzumi, *Chem. Sci.* **2011**, 2, 715; e) S. Fukuzumi, K. Doi, T. Suenobu, K. Ohkubo, Y. Yamada, K. D. Karlin, *Proc. Natl. Acad. Sci. USA* **2012**, DOI: 10.1073/pnas.1119994109.
- [15] a) H. W. Kroto, J. R. Heath, S. C. O'Brien, R. F. Curl, R. E. Smalley, *Nature* **1985**, 318, 162; b) W. Krätschmer, L. D. Lamb, K. Fostiropoulos, D. R. Huffman, *Nature* **1990**, 347, 354; c) R. E. Smalley, *Angew. Chem. Int. Ed. Engl.* **1997**, 36, 1594; d) *Fullerenes, Chemistry, Physics and Technology* (Eds.: K. M. Kadish, R. S. Ruoff), Wiley-Interscience, New York, **2000**.
- [16] a) H. Imahori, K. Tamaki, D. M. Guldi, C. Luo, M. Fujitsuka, O. Ito, Y. Sakata, S. Fukuzumi, *J. Am. Chem. Soc.* **2001**, 123, 2607; b) H. Imahori, D. M. Guldi, K. Tamaki, Y. Yoshida, C. P. Luo, Y. Sakata, S. Fukuzumi, *J. Am. Chem. Soc.* **2001**, 123, 6617; c) H. Imahori, K. Tamaki, Y. Araki, Y. Sekiguchi, O. Ito, Y. Sakata, S. Fukuzumi, *J. Am. Chem. Soc.* **2002**, 124, 5165; d) H. Imahori, Y. Sekiguchi, Y. Kashiwagi, T. Sato, Y. Araki, O. Ito, H. Yamada, S. Fukuzumi, *Chem. Eur. J.* **2004**, 10, 3184; e) D. M. Guldi, H. Imahori, K. Tamaki, Y. Kashiwagi, H. Yamada, Y. Sakata, S. Fukuzumi, *J. Phys. Chem. A* **2004**, 108, 541.
- [17] a) S. Fukuzumi, K. Ohkubo, H. Imahori, J. Shao, Z. Ou, G. Zheng, Y. Chen, R. K. Pandey, M. Fujitsuka, O. Ito, K. M. Kadish, *J. Am. Chem. Soc.* **2001**, 123, 10676; b) K. Ohkubo, H. Imahori, J. Shao, Z. Ou, K. M. Kadish, Y. Chen, G. Zheng, R. K. Pandey, M. Fujitsuka, O. Ito, S. Fukuzumi, *J. Phys. Chem. A* **2002**, 106, 10991; c) K. Ohkubo, H. Kotani, J. G. Shao, Z. P. Ou, K. M. Kadish, G. L. Li, P. K. Pandey, M. Fujitsuka, O. Ito, H. Imahori, S. Fukuzumi, *Angew. Chem.* **2004**, 116, 871; *Angew. Chem. Int. Ed.* **2004**, 43, 853; d) S.-H. Lee, A. G. Larsen, K. Ohkubo, Z.-L. Cai, J. R. Reimers, S. Fukuzumi, M. J. Crossley, *Chem. Sci.* **2012**, 3, 257.
- [18] a) J.-F. Nierengarten, *New J. Chem.* **2004**, 28, 1177; b) F. Langa, M. J. Gomez-Escalonilla, J.-M. Rueff, T. M. Figueira Duarte, J.-F. Nierengarten, V. Palermo, P. Samor, Y. Rio, G. Accorsi, N. Armaroli, *Chem. Eur. J.* **2005**, 11, 4405; c) A. Gégout, J.-F. Nierengarten, B. Delavaux-Nicot, C. Duhayon, A. Saquet, A. Listorti, A. Belbakra, C. Chiorboli, N. Armaroli, *Chem. Eur. J.* **2009**, 15, 8825.
- [19] a) A. Takai, M. Chkouda, A. Eggenspieler, C. P. Gros, M. Lachkar, J.-M. Barbe, S. Fukuzumi, *J. Am. Chem. Soc.* **2010**, 132, 4477; b) F. D'Souza, N. K. Subbaiyan, Y. Xie, J. P. Hill, K. Ariga, K. Ohkubo, S. Fukuzumi, *J. Am. Chem. Soc.* **2009**, 131, 16138; c) F. D'Souza, E. Maligaspe, K. Ohkubo, M. E. Zandler, N. K. Subbaiyan, S. Fukuzumi, *J. Am. Chem. Soc.* **2009**, 131, 8787.
- [20] a) N. Nagata, Y. Kuramochi, Y. Kobuke, *J. Am. Chem. Soc.* **2009**, 131, 10; b) B. Rybtchinski, L. E. Sinks, M. R. Wasielewski, *J. Am. Chem. Soc.* **2004**, 126, 12268; c) F. J. Cspedes-Guirao, K. Ohkubo, S. Fukuzumi, A. Sastre-Santos, F. Fernandez-Lzaro, *J. Org. Chem.* **2009**, 74, 5871; d) M. Ohtani, K. Saito, S. Fukuzumi, *Chem. Eur. J.* **2009**, 15, 9160; e) S. Fukuzumi, K. Saito, K. Ohkubo, T. Khoury, Y. Kashiwagi, M. A. Absalom, S. Gadde, F. D'Souza, Y. Araki, O. Ito, M. J. Crossley, *Chem. Commun.* **2011**, 47, 7980.
- [21] F. D'Souza, G. R. Deviprasad, M. E. Zandler, V. T. Hoang, A. Klydov, M. VanStipdonk, A. Perera, M. E. El-Khouly, M. Fujitsuka, O. Ito, *J. Phys. Chem. A* **2002**, 106, 3243.
- [22] CCDC-888029 (**1a**: C₃₁H₂₈BF₂N₃) contains the supplementary crystallographic data for this paper. These data can be obtained free of charge from The Cambridge Crystallographic Data Centre via www.ccdc.cam.ac.uk/data_request/cif. **1a**: C₃₁H₂₈BF₂N₃; M_w=

- 491.37 g mol⁻¹; triclinic; space group P-1; unit cell dimensions: $a = 9.1410(7)$, $b = 10.1869(8)$, $c = 14.7872(11)$ Å; $\alpha = 99.466(1)$, $\beta = 105.950(1)$, $\gamma = 102.092(1)^\circ$; $V = 1257.96(17)$ Å³; $Z = 2$; $\rho_{\text{calcd}} = 1.297$ Mg m⁻³; absorption coefficient: 0.086 mm⁻¹; Crystal size: 0.35 × 0.23 × 0.07 mm³; Theta range for data collection: 2.10 to 27.04°; reflections collected = 15134; independent reflections = 5493 [$R_{\text{int}} = 0.0243$]; Absorption correction: Semi-empirical from equivalents; $R_1 = 0.0371$ [$I > 2\sigma(I)$]; $R_w = 0.0906$ (all data); GOF = 1.003.
- [23] *Principles of Fluorescence Spectroscopy*, 3rd Ed. (Ed.: J. R. Lakowicz), 2006, Springer, Singapore.
- [24] a) M. Supur, M. E. El-Khouly, J. H. Seok, K.-Y. Kay, S. Fukuzumi, *J. Phys. Chem. A* **2011**, *115*, 14430; b) M. E. El-Khouly, A. G. Moiseev, A. V. der Est, S. Fukuzumi, *ChemPhysChem* **2012**, *13*, 1191.
- [25] H. A. Benesi, J. H. Hildebrand, *J. Am. Chem. Soc.* **1949**, *71*, 2703.
- [26] Gaussian 09, M. J. Frisch, G. W. Trucks, H. B. Schlegel, G. E. Scuseria, M. A. Robb, J. R. Cheeseman, V. G. Zakrzewski, J. A. Montgomery, R. E. Stratmann, J. C. Burant, S. Dapprich, J. M. Millam, A. D. Daniels, K. N. Kudin, M. C. Strain, O. Farkas, J. Tomasi, V. Barone, M. Cossi, R. Cammi, B. Mennucci, C. Pomelli, C. Adamo, S. Clifford, J. Ochterski, G. A. Petersson, P. Y. Ayala, Q. Cui, K. Morokuma, D. K. Malick, A. D. Rabuck, K. Raghavachari, J. B. Foresman, J. Cioslowski, J. V. Ortiz, B. B. Stefanov, G. Liu, A. Liashenko, P. Piskorz, I. Komaromi, R. Gomperts, R. L. Martin, D. J. Fox, T. Keith, M. A. Al-Laham, C. Y. Peng, A. Nanayakkara, C. Gonzalez, M. Challacombe, P. M. W. Gill, B. G. Johnson, W. Chen, M. W. Wong, J. L. Andres, M. Head-Gordon, E. S. Replogle, J. A. Pople, Gaussian, Inc., Pittsburgh, PA, **2009**.
- [27] For a general review on DFT applications of porphyrin-fullerene systems see: M. E. Zandler, F. D'Souza, *C. R. Chimie* **2006**, *9*, 960.
- [28] a) S. Gadde, D. R. Powell, M. E. Zandler, F. D'Souza, *J. Porphyrins Phthalocyanines* **2005**, *9*, 691; b) F. D'Souza, N. P. Rath, G. R. Deviprasad, M. E. Zandler, *Chem. Commun.* **2001**, 267.
- [29] F. D'Souza, M. E. El-Khouly, S. Gadde, A. L. McCarty, P. A. Karr, M. E. Zandler, Y. Araki, O. Ito, *J. Phys. Chem. B* **2005**, *109*, 10107.
- [30] A. Weller, *Z. Phys. Chem. (Muenchen Ger.)* **1982**, *132*, 93.
- [31] M. E. El-Khouly, A. N. Amin, M. E. Zandler, S. Fukuzumi, F. D'Souza, *Chem. Eur. J.* **2012**, *18*, 5239.
- [32] a) E. Maligaspe, T. Kumpulainen, N. K. Subbaiyan, M. E. Zandler, H. Lemmetyinen, N. V. Tkachenko, F. D'Souza, *Phys. Chem. Chem. Phys.* **2010**, *12*, 7434; b) A. Eggenspieler, A. Takai, M. E. El-Khouly, K. Ohkubo, C. P. Gros, C. Bernhard, C. Goze, F. Denat, J.-M. Barbe, S. Fukuzumi, *J. Phys. Chem. A* **2012**, *116*, 3889.
- [33] a) D. M. Guldi, *Chem. Soc. Rev.* **2002**, *31*, 22; b) D. M. Guldi, G. M. A. Rahman, V. Sgobba, C. Ehli, *Chem. Soc. Rev.* **2006**, *35*, 471; c) M. Quintiliani, A. Kahnt, T. Wölfe, W. Hieringer, P. Vázquez, A. Görling, D. M. Guldi, T. Torres, *Chem. Eur. J.* **2008**, *14*, 3765; d) M. S. Rodríguez-Morgade, M. E. Plonska-Brzezinska, A. J. Athans, E. Carbonell, G. de Miguel, D. M. Guldi, L. Echegoyen, T. Torres, *J. Am. Chem. Soc.* **2009**, *131*, 10484.
- [34] a) M. E. El-Khouly, O. Ito, P. M. Smith, F. D'Souza, *J. Photochem. Photobiol. C* **2004**, *5*, 79; b) M. E. El-Khouly, P. Padmawar, Y. Araki, S. Verma, L. Y. Chiang, O. Ito, *J. Phys. Chem. A* **2006**, *110*, 884; c) M. E. El-Khouly, J. H. Kim, M. Kwak, C. S. Choi, O. Ito, K.-Y. Kay, *Bull. Chem. Soc. Jpn.* **2007**, *80*, 2465; d) M. E. El-Khouly, E. S. Kang, K.-Y. Kay, C. S. Choi, Y. Aaraki, O. Ito, *Chem. Eur. J.* **2007**, *13*, 2854; e) M. E. El-Khouly, K.-J. Han, K.-Y. Kay, S. Fukuzumi, *ChemPhysChem* **2010**, *11*, 1726.
- [35] C. A. Wijesinghe, M. E. El-Khouly, N. K. Subbaiyan, M. Supur, M. E. Zandler, K. Ohkubo, S. Fukuzumi, F. D'Souza, *Chem. Eur. J.* **2011**, *17*, 3147.
- [36] F. D'Souza, C. A. Wijesinghe, M. E. El-Khouly, J. Hudson, M. Niemi, H. Lemmetyinen, N. V. Tkachenko, M. E. Zandler, S. Fukuzumi, *Phys. Chem. Chem. Phys.* **2011**, *13*, 18168.

Received: June 26, 2012
Published online: September 20, 2012